UC Davis
UC Davis Previously Published Works

Title

Hydrogen Peroxide Formation in a Surrogate Lung Fluid by Transition Metals and Quinones Present in Particulate Matter

Permalink

https://escholarship.org/uc/item/7wj5c8v9

Journal

Environmental Science and Technology, 48(12)

ISSN

0013-936X

Authors

Charrier, Jessica G
McFall, Alexander S
Richards-Henderson, Nicole K
et al.

Publication Date

2014-06-17

DOI

10.1021/es501011w

Peer reviewed

Hydrogen Peroxide Formation in a Surrogate Lung Fluid by Transition Metals and Quinones Present in Particulate Matter

Jessica G. Charrier,[†] Alexander S. McFall,[‡] Nicole K. Richards-Henderson,[†] and Cort Anastasio*,[†]

[†]Department of Land, Air and Water Resources and [‡]Department of Chemistry, University of California—Davis, 1 Shields Avenue, Davis, California 95616, United States

S *Supporting Information*

ABSTRACT: Inhaled ambient particulate matter (PM) causes adverse health effects, possibly by generating reactive oxygen species (ROS), including hydrogen peroxide (HOOH), in the lung lining fluid. There are conflicting reports in the literature as to which chemical components of PM can chemically generate HOOH in lung fluid mimics. It is also unclear which redox-active species are most important for HOOH formation at concentrations relevant to ambient PM. To address this, we use a cell-free, surrogate lung fluid (SLF) to quantify the initial rate of HOOH formation from 10 transition metals and 4 quinones commonly identified in PM. Copper, 1,2-naphthoquinone, 1,4-naphthoquinone, and phenanthrenequinone all form HOOH in a SLF, but only copper and 1,2-naphthoquinone are likely important at ambient concentrations. Iron suppresses HOOH formation in laboratory solutions, but has a smaller effect in ambient PM extracts, possibly because organic ligands in the particles reduce the reactivity of iron. Overall, copper produces the majority of HOOH chemically generated from typical ambient PM while 1,2-naphthoquinone generally makes a small contribution. However, measured rates of HOOH formation in ambient particle extracts are lower than rates calculated from soluble copper by an average ($\pm 1\sigma$) of $44 \pm 22\%$; this underestimate is likely due to either HOOH destruction by Fe or a reduction in Cu reactivity due to organic ligands from the PM.
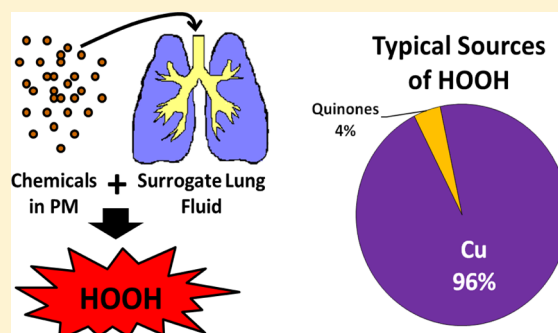
INTRODUCTION

Inhalation of ambient particulate matter (PM) causes respiratory and cardiovascular health problems and mortality in humans.[1−6] PM may induce these effects by producing reactive oxygen species (ROS), including hydrogen peroxide (HOOH) and hydroxyl radical (•OH), in the body.[7,8] Though less reactive than •OH, HOOH is of interest because it is a signaling molecule *in vivo*, has a relatively long lifetime, can cross cell membranes, and is a precursor for •OH.[7,9−11] Once deposited in the lung lining fluid, redox-active species from inhaled PM can chemically produce HOOH at levels that far exceed those originally present in the particles.[12] Endogenous reductants such as ascorbate, and other reducing species such as dithiothreitol (DTT), increase the production of HOOH and •OH from PM or metal solutions;[13−15] thus the interactive chemistry between endogenous reductants and deposited PM can increase the oxidant load in the body.

HOOH occurs naturally in lung fluid and is necessary for proper lung function.[16] However, adverse effects can occur when an overproduction of oxidants—for example, upon PM exposure—overwhelms the body's anti-oxidative defenses.[7,17] It is unclear what concentration of HOOH is necessary to elicit adverse effects in the lung, as HOOH likely affects each cell type differently.[16] Fibroblasts and human alveolar cells exposed to HOOH in the range of 10−400 μM exhibit apoptosis, while higher concentrations induce necrosis.[8,18] Human alveolar and

bronchial epithelial cells released 40% of their lactate dehydrogenase (LDH) in the presence of 100 and 1000 μM HOOH, respectively, indicating alveolar cells may be more susceptible to HOOH than bronchial cells.[19]

Both transition metals (Cu, Zn, Fe) and quinones have been implicated in HOOH formation from PM.[11,13,15,20,21] Zn and Fe were identified via correlation between HOOH production and PM metal content; however, many trace metals and quinones are covariate, which confounds identifying the redox-active species responsible for ROS generation.[21] In addition, although total (acid-soluble) metals are typically measured in these studies, it is likely that the soluble metals drive the redox activity. For example, while ROS production from particles using the dichlorofluorescein diacetate (DCF-DA) assay showed a good correlation between ROS production and soluble Cu ($R^2 = 0.59$), there was no correlation with total Cu ($R^2 = 0.02$).[11] There is also quantitative, mechanistic evidence that specific particle components can generate HOOH. Chung et al.[20] measured quinone concentrations and HOOH production (in the presence of 100 μM DTT) in pH 7.4 aqueous extracts of ambient fine particles (PM$_{2.5}$). Using

concentration−response curves of the pure quinones, they concluded that the quinone content of ambient $PM_{2.5}$ could account for all HOOH produced by the particles. In contrast, Shen et al.[13] found that soluble Cu could explain essentially all HOOH production from ambient fine and coarse PM in pH 7.3 aqueous extracts containing 50 μM ascorbate. Additionally, desferoxamine, a strong metal chelator, halted HOOH production, further indicating that HOOH was produced by metals.

Given the uncertainties in our understanding of HOOH production from ambient PM, our purpose is to quantify HOOH formation from transition metals and quinones (both individually and in mixtures) in a more representative (though still cell-free) surrogate lung fluid (SLF). In this work we characterize an in vitro, cell-free assay to measure the rate of HOOH production from PM. Given the important role of lung-lining fluid antioxidants in ROS formation, we include typical lung concentrations[22] of four antioxidants: ascorbate (Asc), reduced glutathione (GSH), urate (UA), and citrate (Cit). Asc, GSH, and UA are naturally occurring in the lung fluid,[22] while Cit is a good proxy for proteins that mobilize iron in the lung fluid.[23,24] While we use pH and antioxidant conditions similar to lung lining fluid, it is impossible to reproduce the complexity of particle−lung interactions using an in vitro assay. This technique is intended as a useful screening assay for the oxidative potential of ambient PM. It also allows us to identify the chemicals that can produce HOOH in lungs and which of these redox-active species are likely most important for HOOH production from inhaled ambient PM. This complements past work where we quantified •OH formation under the same SLF conditions.[14]

■ EXPERIMENTAL SECTION

Information about chemicals and their purities, metal and quinone stocks, detailed HOOH measurement steps, and ambient PM samples is given in the Supporting Information, section S1.

Surrogate Lung Fluid. Our SLF consists of phosphate-buffered saline (PBS) with four antioxidants. The PBS contains 114 mM NaCl, 7.8 mM sodium phosphate dibasic, and 2.2 mM potassium phosphate monobasic, pH 7.2−7.4, and is treated with Chelex 100 resin (sodium form, Bio-Rad) to remove trace metals.[25,26] Each batch of PBS is treated twice with Chelex resin at a rate of one drop per four seconds. Antioxidant stock solutions, made fresh each day, are added to the PBS at the start of the reaction at final concentrations of 200 μM L-ascorbic acid sodium salt (Asc), 300 μM citric acid (Cit), 100 μM reduced L-glutathione (GSH), and 100 μM uric acid sodium salt (UA).

Quantification of HOOH. We quantify HOOH using the HPLC-fluorescence method described previously.[13,27] Analytical details are given in the Supporting Information, section S1. At time zero, we mix the redox-active species into 5.0 mL of SLF in a 7.0 mL FEP bottle, seal it, and agitate it on a shake table at setting 5 at room temperature. We measure the HOOH concentrations in each reaction solution at 0, 0.5, 1, and 1.5 h. At each time point we remove a 0.50 mL aliquot, add 10.0 μL of 5.0 mM desferoxamine (DSF) to chelate metals and help stabilize the HOOH, and then immediately inject onto the HPLC (50 μL sample loop).

Fe(II) destroys HOOH via the Fenton reaction,[28] and our method is especially sensitive to Fe contamination because of the presence of Asc, which cycles inactive Fe(III) into active

Fe(II). To mitigate this effect, we adhere to rigorous cleaning methods to maintain background Fe concentrations below 50 nM; however, Fe likely destroys some HOOH even at these low levels. We use only FEP bottles (Fisher Scientific), and all are washed in a freshly made 1 M nitric acid bath before use.

Data Analysis and Statistics. We calculate the rate of HOOH production from the concentrations of HOOH measured at 0, 0.5, 1, and 1.5 h. In many cases the rate of HOOH production decreases with time, causing a slight curvature for most data (Figure S1) and significant curvature for solutions with high concentrations of Fe (Figure S2). Similar behavior was observed by Shen et al.[13] for both ambient PM and Cu stocks, and by Wang et al.[21] for HOOH production from coarse mode PM. We calculate the initial rate of HOOH production using the b term of a second-order polynomial: $y = at^2 + bt + c$, where a, b, and c are fitted constants.[21] The initial rate of production between 0 and 1.5 h would not be affected by the choice of reaction time for samples with slight curvature, but could be affected for highly curved samples (generally above 300 nM Fe(II), as shown in Figure S2) if curvature occurs very early. However, significant curvature occurs only for laboratory samples where the rate of HOOH production is essentially zero. Ambient samples did not show as much sensitivity to Fe,[29] as discussed below, and ambient rates should be less sensitive to the choice of time points.

We measure HOOH production in a positive control (250 nM Cu(II)) and blank (SLF containing four antioxidants) on each experiment day. All sample rates are blank-corrected by subtracting that day's blank rate. If data have an error bar it indicates that two or more replicates were measured and the data are reported as the average ± standard deviation of the blank-corrected initial rates. A small subset of data do not have replicates and are reported without an error bar to identify that only one measurement was made. We could estimate the error from the standard error of the slope of the rate regression, but this under-predicts the actual variability of day-to-day replicates. We estimate that the typical relative standard deviation for our rates is 14% based on variability in the blank-corrected positive control, which has an average (±1σ) initial rate of HOOH formation of 1.99 ± 0.28 μM/h ($n = 18$), with a blank rate of 0.21 ± 0.1 μM/h. Statistical differences between means (where $n \geq 2$) are calculated using the student's t-test, with $p \leq 0.05$.

■ RESULTS AND DISCUSSION

HOOH Production from Individual Chemicals. As a first step in identifying the components in PM that can produce HOOH, we start by screening HOOH formation from individual chemicals at a concentration of 500 nM in the SLF. As detailed in the Supporting Information, section S2, 500 nM is a reasonable concentration for Fe and Cu but is over an order of magnitude higher than expected for the quinones (Table S2). We start with this relatively high concentration in order to identify any compound that can produce HOOH under our reaction conditions.

Of the 10 transition metals tested, only Cu(II) produces significant HOOH under our SLF conditions, while Fe(II) destroys background HOOH, resulting in a slightly negative rate of HOOH production (Figure 1). Pb produces HOOH at a rate statistically different than the blank, though extremely slowly. The other seven metals—Mn, Co, V, Ni, Zn, Cd, Cr—do not produce HOOH, though there is some evidence that V can destroy HOOH. Of the four quinones tested, three produce HOOH—phenanthrenequinone (PQN), 1,4-naphthoquinone
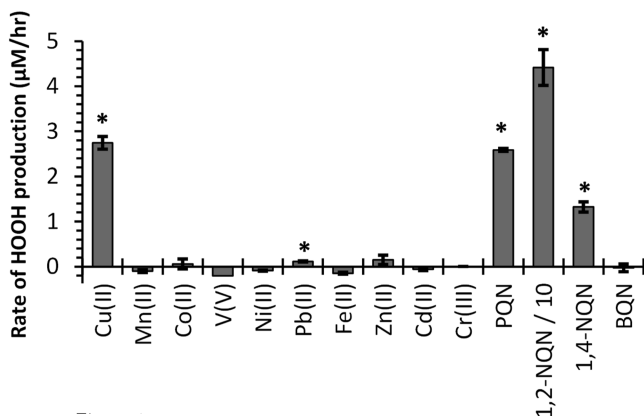
Figure 1. Initial rates of HOOH production from 500 nM concentrations of individual metals and quinones in a SLF with four antioxidants. Error bars represent one standard deviation of replicates ($n \geq 2$). Asterisks mark rates that are statistically larger than zero ($p < 0.05$). The rate for 1,2-NQN ($44 \pm 4 \ \mu M/h$) is divided by 10 to fit on this scale.

(1,4-NQN), and 1,2-naphthoquinone (1,2-NQN)—but benzoquinone (BQN) does not. Previous measurements of HOOH production from 12 quinones in a pH 7.4 extract solution containing 100 μM DTT as a reductant also found that the same three quinones produce HOOH, while the nine other quinones did not.[20] At 500 nM, 1,2-NQN produces 16−33 times more HOOH than an equal concentration of Cu(II), PQN, or 1,4-NQN (Figure 1).

HOOH Concentration−Response Curves. To quantify HOOH production from Cu and quinones at concentrations relevant to ambient PM, we next measured HOOH rates as a function of concentration for the four active compounds. As shown in Figure 2, the concentration responses of all three
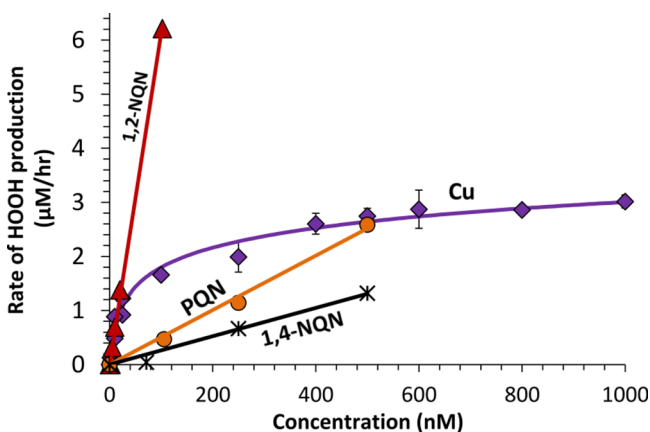
Figure 2. Concentration−response curves of the rates of HOOH production as a function of concentration of redox-active species. Regression equations for the species are given in Table 1

quinones are linear, with slopes (Table 1) that indicate their relative ability to produce HOOH. The relative reactivities of the quinones in our SLF are 23:2:1, i.e., 1,2-NQN ≫ PQN > 1,4-NQN. A previous study by Chung et al. of HOOH production from quinones in pH 7.4 phosphate buffer with 100 μM DTT as a reductant showed a different relative reactivity, PQN > 1,4-NQN = 1,2-NQN.[20] This difference is likely due to the difference in antioxidant composition and reductant. Our SLF uses Asc as the reductant and contains three other

Table 1. Empirical Regression Equations for HOOH Concentration−Response Curves

compd	equation[a]	R^2	concn range (nM)	no. of concns tested
Cu	$Y = 0.524 \ln(X) - 0.615$	0.98	3.4−1000[b]	11
PQN	$Y = 0.0050X$	0.99	0−500	4
1,2-NQN	$Y = 0.061X$	0.998	0−100	6
1,4-NQN	$Y = 0.0026X$	0.98	0−500	4

[a]Y is the initial rate of HOOH production ($\mu M/h$), and X is the concentration of chemical species (nM). [b]HOOH production from Cu goes to zero at 3.4 nM; therefore, HOOH production should be assumed to be zero at Cu concentrations below 3.4 nM. Rates at lower Cu concentrations are indistinguishable from the blank in our experiments.

antioxidants, while Chung et al. used a PBS that contains only DTT. The reductive potential of DTT (-0.33 V)[30] is much stronger than that of Asc ($+0.105$),[31] and our antioxidant composition affects HOOH production (see next section). We have previously shown that PQN is much more active in the DTT assay relative to Cu than in our SLF.[25] When both species are at a concentration of 500 nM, PQN produces the same rate of HOOH production as Cu (Figure 1), while at the same concentration PQN causes 9 times more DTT loss than Cu.[25]

Unlike the quinones, Cu shows a nonlinear concentration response with a fast initial increase in HOOH production that begins to level off around 200 nM Cu (Figure 2). We believe this results from the loss of Asc over time, which causes Asc to become the limiting reactant. As we will describe below (Figure 3) Asc acts as a reductant and is necessary for formation of both
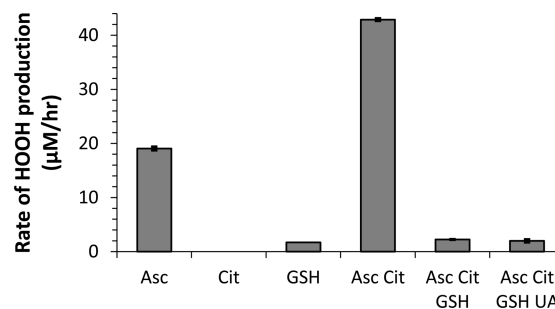
Figure 3. Effect of antioxidant composition on the rate of HOOH production from 250 nM Cu(II) in pH 7.3 PBS. When present, the concentration of each antioxidant is constant for all experiments: Asc is 200 μM, Cit is 300 μM, and GSH and UA are each 100 μM. The final solution composition, with all four antioxidants, is our SLF condition used in all other figures. Each sample rate is corrected by a blank containing the same composition of antioxidants.
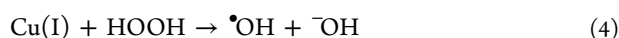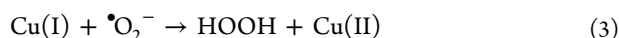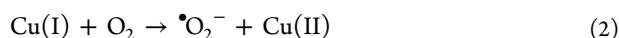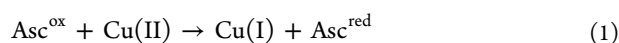
HOOH and •OH in our SLF. Once Asc becomes limiting, addition of more Cu causes only small increases in the rate of HOOH production. A result of the nonlinear behavior is that the relative reactivity of Cu compared to quinones changes depending on the concentrations of each compound in solution. We found a similarly nonlinear concentration−response curve for Cu in the DTT assay, which measures the oxidative potential of PM by monitoring the oxidation of DTT over time.[25] Thus, this result is not limited to the SLF experimental conditions in the HOOH assay. Previous laboratory studies measured the concentration−response curve for HOOH production from Cu(II) in a SLF containing only 50 μM Asc was linear through 400 nM Cu but began to

plateau at 600 nM Cu, the maximum concentration tested.[32] This indicates that the antioxidant mixture in the SLF alters the concentration−response behavior. One implication of the nonlinear Cu curve in Figure 2 is that after 200 nM, large increases in Cu concentration cause only small increases in the rate of HOOH production. At low concentrations (<50 nM), Cu and 1,2-NQN have very similar reactivities, while at higher concentrations 1,2-NQN is much more reactive than Cu. However, this is tempered by the differences in particle concentrations of these two species: For typical ambient conditions (Table S2), the concentration of Cu in a SLF extract of PM will be approximately 100−1000 times larger than that of 1,2-NQN. Therefore, Cu should dominate HOOH production from ambient PM. While filter-based quinone measurements may have both negative (volatilization) and positive (formation from ozone) artifacts,[20] the magnitudes of these artifacts are unlikely to be large enough to make 1,2-NQN more significant than Cu as a source of HOOH for typical ambient PM.

Effect of Antioxidants on HOOH Production. Our SLF includes four antioxidants: Asc, Cit, GSH, and UA. In previous work using the same SLF we found that the antioxidant composition has a significant effect on •OH production from transition metals.[14] Because HOOH is a precursor for •OH, we expect that these antioxidants also affect HOOH production. We test different mixtures of antioxidants to better characterize our assay; however, the base case is a SLF with all four antioxidants. This base case is used for all experiments excluding Figure 3.

As expected, HOOH production by 250 nM Cu is affected by the antioxidant composition (Figure 3). Cu produces HOOH in the presence of Asc, and to a much smaller extent in the presence of GSH only, but not in the presence of Cit only. Asc acts as the reductant in our system, cycling transition metals from their oxidized to reduced forms and thereby allowing oxidant production from Cu(II) via pathways such as

$$Asc^{ox} + Cu(II) \rightarrow Cu(I) + Asc^{red} \tag{1}$$

$$Cu(I) + O_2 \rightarrow {}^{\bullet}O_2^{-} + Cu(II) \tag{2}$$

$$Cu(I) + {}^{\bullet}O_2^{-} \rightarrow HOOH + Cu(II) \tag{3}$$

$$Cu(I) + HOOH \rightarrow {}^{\bullet}OH + {}^{-}OH \tag{4}$$

Although Cu with GSH produces HOOH (Figure 3), this mixture does not form •OH.[14] Compared to Asc only, the combination of Asc and Cit doubles the rate of HOOH production, to 43 μM/h for 250 nM Cu(II). Under the conditions with Asc and Cit as the only antioxidants, 100% of Cu(II) is bound to Cit.[14] Thus, the Cu(II)-citrate complex is apparently more reactive than free Cu(II), which is the dominant Cu form in the Asc-only condition.[14] If we add GSH to the Asc Cit mixture, the production of HOOH plummets by a factor of 20, to 2.2 μM/h, which is similar to the HOOH production rate from our SLF case with all four antioxidants. Thus, UA does not affect HOOH production from Cu in the presence of the other antioxidants. Overall, HOOH production in our mixture with all four antioxidants is substantially reduced because of GSH, likely because GSH binds to Cu and reduces its reactivity. A similar suppression by GSH was observed for •OH production from Cu(II) in the same SLF,[14] and also in other studies of •OH from Cu.[33,34] MINTEQ speciation modeling of a similar SLF with the same four antioxidants

shows that GSH replaces Cit as the primary ligand, and 100% of Cu(II) is bound to GSH under these conditions.[14] GSH is well known as an important antioxidant *in vivo*, and may be especially important in mitigating damage from HOOH.[19] Binding and deactivating Cu may be one component of this protective effect of GSH.

We also find that the antioxidant mixture affects the ability of quinones to generate HOOH. As shown in Figure S3, compared to the case of Asc only, HOOH production in the four antioxidant (SLF) mixture is lower by factors of 2 and 6 for 500 nM PQN and 20 nM 1,2-NQN, respectively. While HOOH formation from the quinones is less sensitive to antioxidant composition than is Cu, the impact on quinones is surprising and more work is necessary to confirm this result and understand its mechanism.

HOOH Production from Mixtures of Metals and Quinones. Ambient PM samples contain a complex mixture of chemical species that may produce HOOH in a more complicated mechanism than in the pure laboratory solutions measured here. For example, quinones and Cu can act synergistically to produce HOOH under some conditions: semiquinone radicals can reduce Cu(II) to Cu(I), producing superoxide that can react with Cu(I) to make HOOH.[15,35] To examine this in our SLF, we measured HOOH production in mixtures of Cu, quinones, and/or Fe (Figure 4). The gray bars
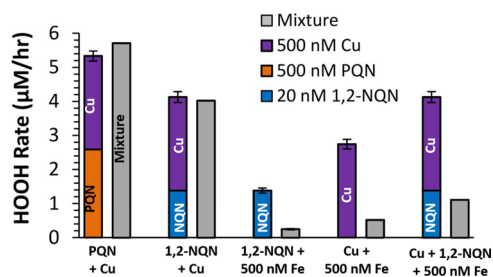
Figure 4. Initial rates of HOOH production in laboratory mixtures of quinones and/or transition metals (gray bars) compared to the sum of the rates from the individual redox-active species (stacked colored bars). Error bars of the colored stacked bars are the propagated errors of the sum (all have replicate samples). The concentrations of metals and quinones are constant: Cu, Fe, and PQN are at 500 nM, and 1,2-NQN is at 20 nM.

in Figure 4 represent the rate of HOOH production measured from the species mixed in the same bottle, while the colored stacked bars are the sum of HOOH production measured from the individual compounds.

As shown by the first two sets of bars, the rate of HOOH production in a mixture of a quinone and Cu is the same as the sum of the rates of the individual species; i.e., HOOH production from Cu and either 1,2-NQN or PQN is additive (Figure 4). Thus, reactions between Cu and quinones appear to be negligible for HOOH formation in this system. This may be due to the presence of Asc, which rapidly cycles Cu(II) to Cu(I) and is present at a concentration that is 400−10,000 times higher than the quinones; we expect a similar Asc dominance in lung lining fluid in vivo. This likely causes most Cu(II) to react with Asc instead of a semiquinone radical. In contrast to the additive behavior of Cu with quinones, the addition of 500 nM Fe to SLF containing Cu and/or 1,2-NQN, greatly reduces HOOH formation, to 20−30% of the rate measured without Fe (Figure 4). This decrease in the rate of HOOH formation might be because Fe is suppressing the
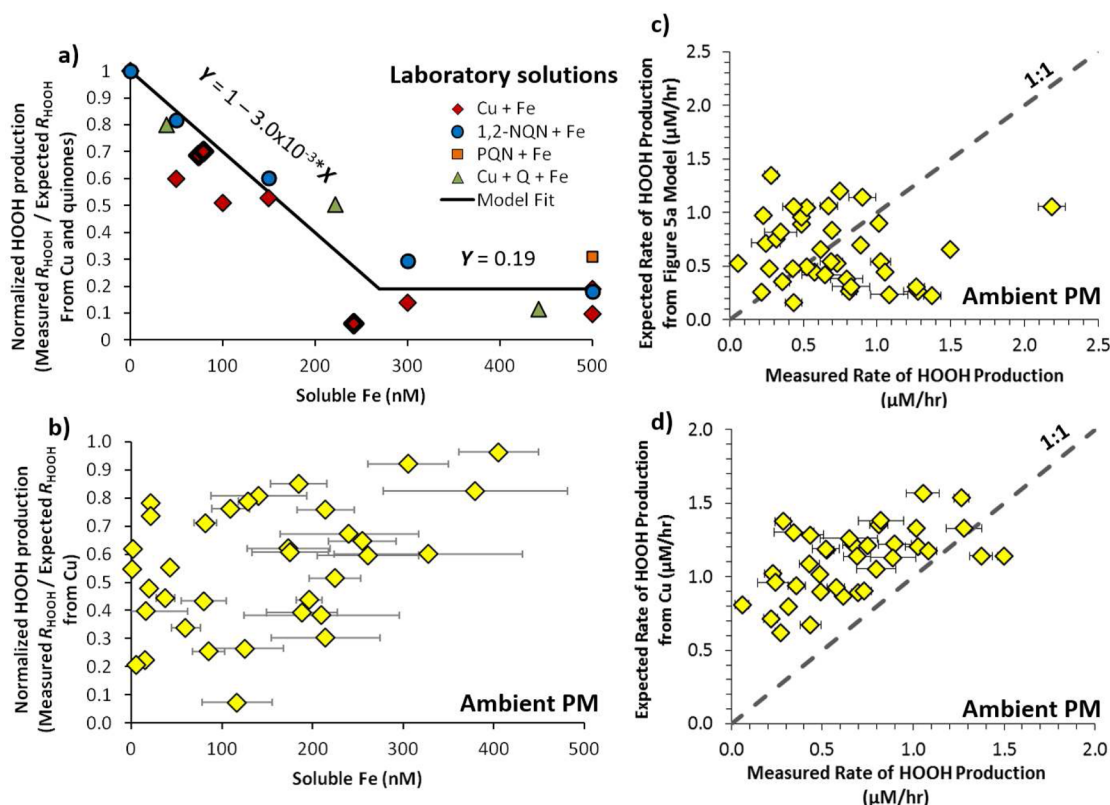
Figure 5. Impact of iron on HOOH production in laboratory solutions and suppression of HOOH production in extracts of ambient particles. Panel (a) shows the normalized HOOH production, i.e., the measured rate of HOOH formation in laboratory mixtures containing copper and/or quinones and iron divided by the expected (calculated) rate from just the copper and quinones. The rate of HOOH production in the absence of Fe is measured directly for all cases except the three diamonds marked with a bold outline, where HOOH production was calculated based on the concentration of Cu. Black lines in panel (a) are the model fits to the data, with equations noted on the lines. Panel (b) shows the normalized HOOH production for ambient particle extracts from Fresno, CA, where the expected rate was calculated using only the copper concentration. The last two panels compare the measured rates of HOOH production in ambient PM extracts with (c) the calculated HOOH rates based on the fit to the laboratory solutions in panel (a), and (d) the calculated rates based only on the concentrations of soluble Cu in the ambient PM extracts.

formation of HOOH from Cu or quinones, or because Fe(II) is destroying HOOH and converting it to $^\bullet$OH via the Fenton reaction. We cannot deduce which mechanism is at work here, but plan to explore this in the future by looking at $^\bullet$OH production from the same mixtures. Based on these results, Fe may have an important role in suppressing HOOH generation in ambient PM extracts since ambient concentrations of Fe are high, resulting in SLF concentrations up to a few micromolar under the sampling conditions described in the Supporting Information, section S2.

Suppression of HOOH Production by Fe. We further investigated the effect of Fe by quantifying HOOH production in 17 laboratory solutions containing mixtures of Fe with Cu, 1,2-NQN,1,4-NQN and/or PQN (summarized in Table S3). We express the impact of Fe in Figure 5a using the "normalized HOOH production rate", which is a value between 0 and 1 calculated according to

$$\text{Normalized HOOH production} = \frac{(\text{Measured HOOH rate})}{(\text{Expected HOOH rate without Fe})} \quad \text{(R1)}$$

The numerator is the measured HOOH rate in the mixture (including Fe), while the denominator is the HOOH rate in the absence of Fe, which was either measured directly or determined based on the Cu and/or quinone concentrations

in conjunction with the concentration−response curves in Table 1. As an example, a normalized HOOH production value of 0.7 indicates the HOOH rate in the presence of Fe is 70% of the rate in a similar solution without Fe (i.e,. there is a 30% suppression by Fe).

Figure 5a shows that Fe has a similar effect on all of the laboratory mixtures: the normalized rate of HOOH production decreases with increasing Fe concentration between 0 and 270 nM and is relatively stable—at approximately 20% of the rate in the absence of Fe—at higher Fe concentrations. We applied the same analysis to 39 ambient samples collected in Fresno, CA, during 2008 and 2009.[36] We measured both the concentration of soluble metals and the initial rate of HOOH production from these samples, but did not measure the concentration of quinones (Supporting Information, section S1).[29] We calculate the normalized rate of HOOH production from the ambient extracts using the expected rate from soluble Cu since quinone concentrations are unknown (Figure 5b). Compared to the laboratory mixtures, Fe appears to have nearly the opposite effect on HOOH production in the ambient PM extracts: there is generally less suppression of HOOH formation as the concentration of Fe increases (Figure 5b), but the relationship is very scattered and there is no strong trend. How could higher concentrations of Fe lead to a smaller suppression of HOOH production by Fe? One possibility is that samples with higher Fe concentrations also contain higher amounts of organic

ligands, which are binding to Fe and reducing its ability to reduce HOOH formation. In our laboratory solutions Cit is the dominant ligand for Fe[14] and the Fe-Cit complex clearly suppresses HOOH formation (Figure 5a). It is also possible that Cu produces HOOH less efficiently in ambient samples compared to in our laboratory solutions due to the presence of organic ligands (Figure 2).

If we apply the laboratory solutions model from Figure 5a to ambient PM we can calculate the expected HOOH production based on the concentration of Cu and Fe in each sample. When we plot the measured versus expected HOOH production using this method (Figure 5c), the modeled data are clustered around the 1:1 line, but the R^2 value for this correlation is 0.01, indicating the model has no predictive ability. We obtain a much better relationship ($R^2 = 0.3$) when we calculate the expected rate of HOOH production based on only the concentration of soluble Cu using the Cu concentration–response curve (Figure 2), without considering suppression by Fe (Figure 5d). In this case the expected rate of HOOH production is nearly always larger than the measured rate (i.e., points are almost all above the 1:1 line). This overestimate of HOOH rates suggests HOOH production is suppressed in ambient PM extracts, but that this suppression is not strongly tied to the soluble Fe concentration. It is also possible that organic ligands from the particles are binding to Cu and suppressing its ability to form HOOH. If we assume that Cu controls HOOH formation in Figure 5d (i.e., if the contribution from quinones is negligible), the average ($\pm 1\sigma$) suppression in HOOH formation by Cu in ambient PM extracts is $44 \pm 22\%$ (median suppression = 40%; range = 3.7–93%. More work is needed to determine whether this suppression is due to Fe or to a reduction in Cu reactivity by organic ligands, but the chemistry of HOOH production in ambient particles is clearly complicated. However, the similarity between the measured rate of HOOH production and that predicted by Cu (Figure 5d) indicates that Cu is likely a major contributor to HOOH production.

Implications for HOOH Formation from Ambient PM. Because of the variable impact of Fe on HOOH production in ambient PM extracts, and the potential for particulate ligands to reduce Cu reactivity, we cannot predict the absolute rate of HOOH production based on the concentration of soluble metals in ambient PM. However, mixtures of Cu and quinones (the only species able to make HOOH based in Figure 1) show that the rate of HOOH production from these redox-active species is additive (Figure 4) and that Fe has a similar suppressive effect on HOOH production from both species (Figure 5a). Thus, in the case that Fe is responsible for suppressing HOOH in ambient PM extracts we can still estimate the "unsuppressed" rate of HOOH production based on the reported range of ambient $PM_{2.5}$ quinone and soluble Cu concentrations (Table S2). Under these conditions Cu produces the largest rate of HOOH production, 0.8 to 2.9 μM HOOH per hour, across the entire range of redox-active concentrations reported in the literature. Quinones, on the other hand, exhibit very low particle-phase concentrations and generally do not contribute significantly to HOOH production. At the highest ambient concentrations, 1,2-NQN can produce on the order of 0.5 μM HOOH per hour, while the rates for 1,4-NQN and PQN are in the range 0.0–0.05 μM/h, which is negligible compared to production from Cu. If we consider the lowest, median, and highest concentrations of each redox-active species, Cu accounts for nearly all HOOH production (100%,

96%, and 84%, respectively), while 1,2-NQN accounts for 0%, 2%, and 14% of total HOOH for these three scenarios, while the other quinones make up the remainder. Though the total HOOH rate in ambient PM extracts will be somewhat lower than these calculated rates, these results indicate Cu will dominate HOOH production in ambient PM.

We also consider the possibility that reduced Cu reactivity (rather than reactions with Fe) accounts for the HOOH suppression we see in ambient PM extracts (Figure 5). In this case we repeat the rate calculations above but with a 44% reduction in the rate of HOOH formation by Cu, which is the average reduction needed to explain Figure 5d. In this case, Cu is still the dominant source of HOOH in PM extracts, accounting for 100%, 93%, and 75% of HOOH formation for the lowest, median, and highest concentration scenarios. Thus, even if Cu reactivity is suppressed in ambient PM, we expect soluble Cu to dominate HOOH production in most ambient PM samples.

This result agrees with other studies that have identified Cu as important for ROS generation using a variety of techniques, including the DTT assay,[25,37] a macrophage ROS assay,[38,39] and HOOH and •OH measurements.[13,32,40,41] These results also agree with a recent epidemiological study that found the Cu content of PM was associated with mortality in California.[3] One important source of Cu is likely traffic emissions,[42,43] which have been consistently linked to adverse health effects.[44–47] For example, rats instilled with particles from multiple sites showed a statistically significantly higher response for sites with higher traffic emissions and a higher concentration of Cu, but no association with the PAH content of PM.[48] Taken together, these diverse studies provide consistent evidence that Cu is an important component in the health effects from airborne particles.

■ ASSOCIATED CONTENT

ⓢ Supporting Information

Additional methods, four figures, and three tables that contain data referenced in the main text. This material is available free of charge via the Internet at http://pubs.acs.org.

■ AUTHOR INFORMATION

Corresponding Author

*Phone: (530) 754-6095; fax: (530) 752-1552; e mail: canastasio@ucdavis.edu.

Notes

■ ACKNOWLEDGMENTS

to J.G.C. (FP-917181), and the California Agricultural Experiment Station (Project CA-D*-LAW-6403-RR).

■ REFERENCES

(1) Pope, C. A.; Thun, M. J.; Namboodiri, M. M.; Dockery, D. W.; Evans, J. S.; Speizer, F. E.; Heath, C. W. Particulate air pollution as a predictor of mortality in a prospective study of US adults. *Am. J. Respir. Crit. Care Med.* **1995**, *V151* (N3), 669−674.

(2) Dockery, D. W.; Pope, C. A.; Xu, X. P.; Spengler, J. D.; Ware, J. H.; Fay, M. E.; Ferris, B. G.; Speizer, F. E. An association between air pollution and mortality in 6 United-States cities. *N. Engl. J. Med.* **1993**, *329* (24), 1753−1759.

(3) Ostro, B.; Feng, W.-Y.; Broadwin, R.; Green, S.; Lipsett, M. The effects of components of fine particulate air pollution on mortality in California: Results from CALFINE. *Environ. Health Perspect.* **2007**, *115* (1), 13−19.

(4) Lall, R.; Ito, K.; Thurston, G. Distributed lag analyses of daily hospital admissions and source-apportioned fine particle air pollution. *Environ. Health Perspect.* **2011**, *119* (4), 455−460.

(5) Samet, J. M.; Dominici, F.; Curriero, F. C.; Coursac, I.; Zeger, S. L. Fine particulate air pollution and mortality in 20 US Cities, 1987−1994. *N. Engl. J. Med.* **2000**, *343* (24), 1742−1749.

(6) Dominici, F.; Peng, R. D.; Bell, M. L.; Pham, L.; McDermott, A.; Zeger, S. L.; Samet, J. M. Fine particulate air pollution and hospital admission for cardiovascular and respiratory diseases. *JAMA—J. Am. Med. Assoc.* **2006**, *295* (10), 1127−1134.

(7) Li, N.; Hao, M. Q.; Phalen, R. F.; Hinds, W. C.; Nel, A. E. Particulate air pollutants and asthma—A paradigm for the role of oxidative stress in PM-induced adverse health effects. *Clin. Immunol.* **2003**, *109* (3), 250−265.

(8) Geiser, T.; Ishigaki, M.; van Leer, C.; Matthay, M. A.; Broaddus, V. C. H_2O_2 inhibits alveolar epithelial wound repair in vitro by induction of apoptosis. *Am. J. Physiol.—Lung, Cell., Mol. Physiol.* **2004**, *287* (2), L448−L453.

(9) Wilhelm, J.; Vankova, M.; Maxova, H.; Siskova, A. Hydrogen peroxide production by alveolar macrophages is increased and its concentration is elevated in the breath of rats exposed to hypoxia: Relationship to lung lipid peroxidation. *Physiol. Res.* **2003**, *52* (3), 327−332.

(10) Waghray, M.; Cui, Z. B.; Horowitz, J. C.; Subramanian, I. M.; Martinez, F. J.; Toews, G. B.; Thannickal, V. J. Hydrogen peroxide is a diffusible paracrine signal for the induction of epithelial cell death by activated myofibroblasts. *FASEB J.* **2005**, *19* (2), 854−+.

(11) See, S. W.; Wang, Y. H.; Balasubramanian, R. Contrasting reactive oxygen species and transition metal concentrations in combustion aerosols. *Environ. Res.* **2007**, *103* (3), 317−324.

(12) Arellanes, C.; Paulson, S. E.; Fine, P. M.; Sioutas, C. Exceeding of Henry's law by hydrogen peroxide associated with urban aerosols. *Environ. Sci. Technol.* **2006**, *40* (16), 4859−4866.

(13) Shen, H.; Barakat, A. I.; Anastasio, C. Generation of hydrogen peroxide from San Joaquin Valley particles in a cell-free solution. *Atmos. Chem. Phys.* **2011**, *11* (2), 753−765.

(14) Charrier, J. G.; Anastasio, C. Impacts of antioxidants on hydroxyl radical production from individual and mixed transition metals in a surrogate lung fluid. *Atmos. Environ.* **2011**, *45* (40), 7555−7562.

(15) Wang, Y.; Arellanes, C.; Paulson, S. E. Hydrogen peroxide associated with ambient fine-mode, diesel, and biodiesel aerosol particles in Southern California. *Aerosol Sci. Technol.* **2012**, *46* (4), 394−402.

(16) Oosting, R. S.; Vanbree, L.; Vaniwaarden, J. F.; Vangolde, L. M. G.; Verhoef, J. Impairment of Phagocytic Functions of Alveolar Macrophages by Hydrogen-Peroxide. *Am. J. Physiol.* **1990**, *259* (2), L87−L94.

(17) Li, N.; Xia, T.; Nel, A. E. The role of oxidative stress in ambient particulate matter-induced lung diseases and its implications in the toxicity of engineered nanoparticles. *Free Radic. Biol. Med.* **2008**, *44* (9), 1689−1699.

(18) Teramoto, S.; Tomita, T.; Matsui, H.; Ohga, E.; Matsuse, T.; Ouchi, Y. Hydrogen peroxide-induced apoptosis and necrosis in human lung fibroblasts: Protective roles of glutathione. *Jpn. J. Pharmacol.* **1999**, *79* (1), 33−40.

(19) Mulier, B.; Rahman, I.; Watchorn, T.; Donaldson, K.; MacNee, W.; Jeffery, P. K. Hydrogen peroxide-induced epithelial injury: the protective role of intracellular nonprotein thiols (NPSH). *Eur. Respir. J.* **1998**, *11* (2), 384−391.

(20) Chung, M. Y.; Lazaro, R. A.; Lim, D.; Jackson, J.; Lyon, J.; Rendulic, D.; Hasson, A. S. Aerosol-borne quinones and reactive oxygen species generation by particulate matter extracts. *Environ. Sci. Technol.* **2006**, *40* (16), 4880−4886.

(21) Wang, Y.; Arellanes, C.; Curtis, D. B.; Paulson, S. E. Probing the source of hydrogen peroxide associated with coarse mode aerosol particles in Southern California. *Environ. Sci. Technol.* **2010**, *44* (11), 4070−4075.

(22) Cross, C. E.; Vandervliet, A.; Oneill, C. A.; Louie, S.; Halliwell, B. Oxidants, antioxidants, and respiratory-tract lining fluids. *Environ. Health Perspect.* **1994**, *102*, 185−191.

(23) Lund, L. G.; Aust, A. E. Iron mobilization from crocidolite asbestos greatly enhances crocidolite-dependent formation of DNA single-strand breaks in PHI-X174 RFI DNA. *Carcinogenesis* **1992**, *13* (4), 637−642.

(24) Smith, K. R.; Aust, A. E. Mobilization of iron from urban particulates leads to generation of reactive oxygen species in vitro and induction of ferritin synthesis in human lung epithelial cells. *Chem. Res. Toxicol.* **1997**, *10* (7), 828−34.

(25) Charrier, J. G.; Anastasio, C. On dithiothreitol (DTT) as a measure of oxidative potential for ambient particles: evidence for the importance of soluble transition metals. *Atmos. Chem. Phys. Discuss.* **2012**, *12*, 8533−8546.

(26) Bio-Rad. Chelex 100 and Chelex 20 chelating ion exchange resin instruction manual. http://www.bio-rad.com/webmaster/pdfs/9184_Chelex.PDF, 1991.

(27) Kok, G. L.; McLaren, S. E.; Staffelbach, T. A. HPLC determination of atmospheric organic hydroperoxides. *J. Atmos. Ocean. Technol.* **1995**, *12* (2), 282−289.

(28) Stohs, S. J.; Bagchi, D. Oxidative mechanisms in the toxicity of metal-ions. *Free Radic. Biol. Med.* **1995**, *18* (2), 321−336.

(29) Richards-Henderson, N. K.; Charrier, J. G.; Bein, K. J.; Bau, D.; Wexler, A. S.; Anastasio, C. Oxidant production from source-oriented particulate matter − Part 2: Hydrogen peroxide and hydroxyl radical. *Atmos. Chem. Phys.* **2014**, submitted.

(30) Cleland, W. W. Dithiothreitol, a new protective reagent for SH groups. *Biochemistry* **1964**, *3* (4), 480−482.

(31) Merkofer, M.; Kissner, R.; Hider, R. C.; Brunk, U. T.; Koppenol, W. H. Fenton chemistry and iron chelation under physiologically relevant conditions: electrochemistry and kinetics. *Chem. Res. Toxicol.* **2006**, *19* (10), 1263−1269.

(32) Shen, H.; Anastasio, C. A comparison of hydroxyl radical and hydrogen peroxide generation in ambient particle extracts and laboratory metal solutions. *Atmos. Environ.* **2012**, *46*, 665−668.

(33) Hanna, P. M.; Mason, R. P. Direct evidence for inhibition of free-radical formation from Cu(I) and hydrogen-peroxide by glutathione and other potential ligands using the EPR spin-trapping technique. *Arch. Biochem. Biophys.* **1992**, *295* (1), 205−213.

(34) Maestre, P.; Lambs, L.; Thouvenot, J. P.; Berthon, G. Copper-ligand interactions and physiological free-radical processes—pH-dependent influence of Cu^{2+} ions on Fe^{2+}-driven OH generation. *Free Radical Res. Commun.* **1992**, *15* (6), 305−317.

(35) Li, Y. B.; Trush, M. A. Oxidation of hydroquinone by copper—chemical mechanism and biological effects. *Arch. Biochem. Biophys.* **1993**, *300* (1), 346−355.

(36) Bein, K. J.; Zhao, Y.; Wexler, A. S. Conditional sampling for source-oriented toxicological studies using a single particle mass spectrometer. *Environ. Sci. Technol.* **2009**, *43* (24), 9445−9452.

(37) Ntziachristos, L.; Froines, J. R.; Cho, A. K.; Sioutas, C. Relationship between redox activity and chemical speciation of size-fractionated particulate matter. *Part. Fibre Toxicol.* **2007**, *4*, (5).

(38) Daher, N.; Ruprecht, A.; Invernizzi, G.; De Marco, C.; Miller-Schulze, J.; Heo, J. B.; Shafer, M. M.; Shelton, B. R.; Schauer, J. J.; Sioutas, C. Characterization, sources and redox activity of fine and coarse particulate matter in Milan, Italy. *Atmos. Environ.* **2012**, *49*, 130−141.

(39) Hu, S.; Polidori, A.; Arhami, M.; Shafer, M. M.; Schauer, J. J.; Cho, A.; Sioutas, C. Redox activity and chemical speciation of size fractioned PM in the communities of the Los Angeles-Long Beach harbor. *Atmos. Chem. Phys.* **2008**, *8* (21), 6439−6451.

(40) Shen, H.; Anastasio, C., Formation of hydroxyl radical from San Joaquin Valley particles extracted in a cell-free surrogate lung fluid. *Atmos. Chem. Phys.* **2011**, *11*, (18).

(41) DiStefano, E.; Eiguren-Fernandez, A.; Delfino, R. J.; Sioutas, C.; Froines, J. R.; Cho, A. K. Determination of metal-based hydroxyl radical generating capacity of ambient and diesel exhaust particles. *Inhal. Tox.* **2009**, *21* (8−11), 731−738.

(42) Lough, G. C.; Schauer, J. J.; Park, J. S.; Shafer, M. M.; Deminter, J. T.; Weinstein, J. P. Emissions of metals associated with motor vehicle roadways. *Environ. Sci. Technol.* **2005**, *39* (3), 826−836.

(43) Hulskotte, J. H. J.; van der Gon, H.; Visschedijk, A. H.; Schaap, M. Brake wear from vehicles as an important source of diffuse copper pollution. *Water Sci. Technol.* **2007**, *56* (1), 223−231.

(44) Gasser, M.; Riediker, M.; Mueller, L.; Perrenoud, A.; Blank, F.; Gehr, P.; Rothen-Rutishauser, B., Toxic effects of brake wear particles on epithelial lung cells in vitro. *Part. Fibre Toxicol.* **2009**, *6*.

(45) Godri, K. J.; Harrison, R. M.; Evans, T.; Baker, T.; Dunster, C.; Mudway, I. S.; Kelly, F. J. Increased Oxidative Burden Associated with Traffic Component of Ambient Particulate Matter at Roadside and Urban Background Schools Sites in London. *PLoS One* **2011**, *6* (7), No. e21961.

(46) Hoek, G.; Brunekreef, B.; Goldbohm, S.; Fischer, P.; van den Brandt, P. A. Association between mortality and indicators of traffic-related air pollution in the Netherlands: a cohort study. *Lancet* **2002**, *360* (9341), 1203−1209.

(47) Hoffmann, B.; Moebus, S.; Mohlenkamp, S.; Stang, A.; Lehmann, N.; Dragano, N.; Schmermund, A.; Memmesheimer, M.; Mann, K.; Erbel, R.; Jockel, K. H. Residential exposure to traffic is associated with coronary atherosclerosis. *Circulation* **2007**, *116* (5), 489−496.

(48) Gerlofs-Nijland, M. E.; Dormans, J.; Bloemen, H. J. T.; Leseman, D.; Boere, A. J. F.; Kelly, F. J.; Mudway, I. S.; Jimenez, A. A.; Donaldson, K.; Guastadisegni, C.; Janssen, N. A. H.; Brunekreef, B.; Sandstrom, T.; Cassee, F. R. Toxicity of coarse and fine particulate matter from sites with contrasting traffic profiles. *Inhal. Tox.* **2007**, *19* (13), 1055−1069.